2. Although their definitions are similar, the Nusselt number is defined in terms of the thermal conductivity of the fluid, whereas the Biot number is defined in terms of the thermal conductivity of the solid.
3. Options for enhancing production rates include accelerating the cooling process by increasing the fluid velocity and/or using a different fluid. Applying the foregoing procedures, the cooling time is computed and plotted for air and helium over the range of velocities, $5 \leq V \leq 25$ m/s.

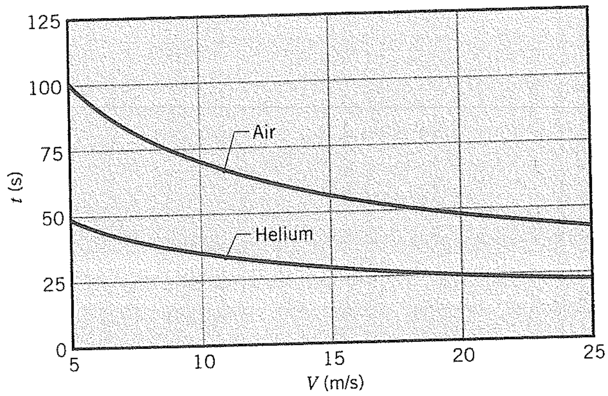

Although Reynolds numbers for He are much smaller than those for air, the thermal conductivity is much larger and, as shown below, convection heat transfer is enhanced.

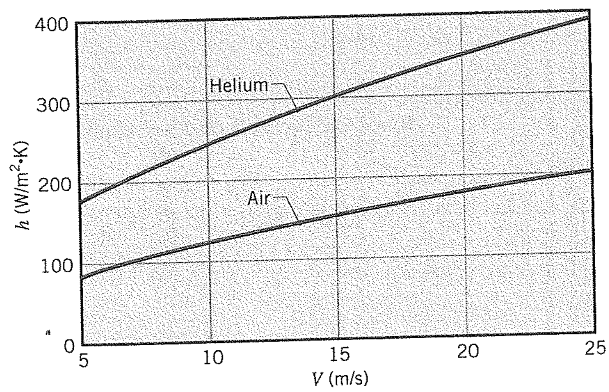

Hence production rates could be increased by substituting helium for air, albeit with a significant increase in cost.

7.6 *Flow across Banks of Tubes*

Heat transfer to or from a bank (or bundle) of tubes in cross flow is relevant to numerous industrial applications, such as steam generation in a boiler or air cooling in the coil of an air conditioner. The geometric arrangement is shown schematically

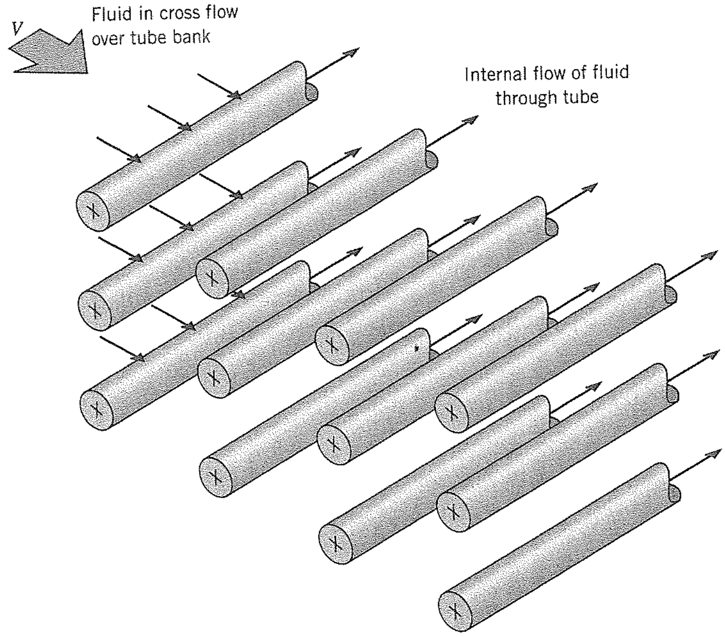

FIGURE 7.10 Schematic of a tube bank in cross flow.

in Figure 7.10. Typically, one fluid moves over the tubes, while a second fluid at a different temperature passes through the tubes. In this section we are specifically interested in the convection heat transfer associated with cross flow over the tubes.

The tube rows of a bank are either *staggered* or *aligned* in the direction of the fluid velocity V (Figure 7.11). The configuration is characterized by the tube diameter D and by the *transverse pitch* S_T and *longitudinal pitch* S_L measured between tube centers. Flow conditions within the bank are dominated by boundary layer separation effects and by wake interactions, which in turn influence convection heat transfer.

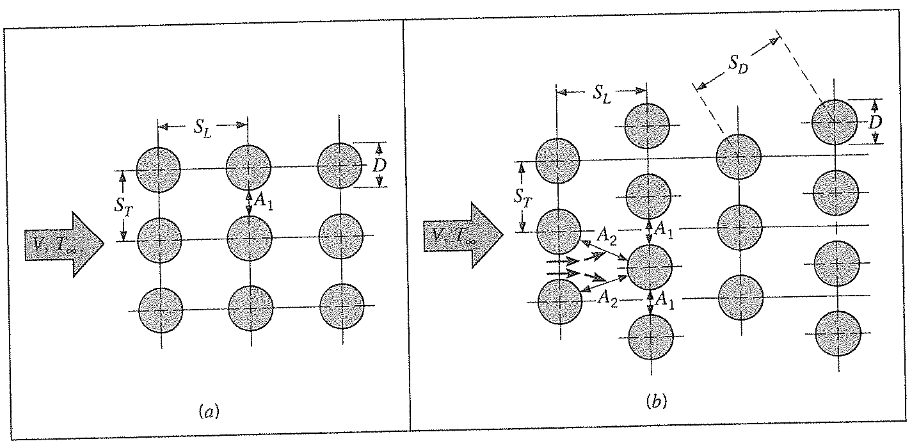

FIGURE 7.11 Tube arrangements in a bank. (*a*) Aligned. (*b*) Staggered.

The heat transfer coefficient associated with a tube is determined by its position in the bank. The coefficient for a tube in the first row is approximately equal to that for a single tube in cross flow, whereas larger heat transfer coefficients are associated with tubes of the inner rows. The tubes of the first few rows act as a turbulence-generating grid, which increases the heat transfer coefficient for tubes in the following rows. In most configurations, however, heat transfer conditions stabilize, such that little change occurs in the convection coefficient for a tube beyond the fourth or fifth row.

Generally, we wish to know the *average* heat transfer coefficient for the *entire* tube bundle. For airflow across tube bundles composed of *10 or more rows* ($N_L \geq 10$), Grimison [19] has obtained a correlation of the form

$$\overline{Nu}_D = C_1 \, Re_{D,\max}^m \quad \begin{bmatrix} N_L \geq 10 \\ 2000 \lesssim Re_{D,\max} \lesssim 40{,}000 \\ Pr = 0.7 \end{bmatrix} \tag{7.58}$$

where C_1 and m are listed in Table 7.5 and

$$Re_{D,\max} \equiv \frac{\rho V_{\max} D}{\mu} \tag{7.59}$$

It has become common practice to extend this result to other fluids through insertion of the factor $1.13 Pr^{1/3}$, in which case

TABLE 7.5 Constants of Equations 7.58 and 7.60 for airflow over a tube bank of 10 or more rows [19]

	S_T/D							
	1.25		1.5		2.0		3.0	
S_L/D	C_1	m	C_1	m	C_1	m	C_1	m
Aligned								
1.25	0.348	0.592	0.275	0.608	0.100	0.704	0.0633	0.752
1.50	0.367	0.586	0.250	0.620	0.101	0.702	0.0678	0.744
2.00	0.418	0.570	0.299	0.602	0.229	0.632	0.198	0.648
3.00	0.290	0.601	0.357	0.584	0.374	0.581	0.286	0.608
Staggered								
0.600	—	—	—	—	—	—	0.213	0.636
0.900	—	—	—	—	0.446	0.571	0.401	0.581
1.000	—	—	0.497	0.558	—	—	—	—
1.125	—	—	—	—	0.478	0.565	0.518	0.560
1.250	0.518	0.556	0.505	0.554	0.519	0.556	0.522	0.562
1.500	0.451	0.568	0.460	0.562	0.452	0.568	0.488	0.568
2.000	0.404	0.572	0.416	0.568	0.482	0.556	0.449	0.570
3.000	0.310	0.592	0.356	0.580	0.440	0.562	0.428	0.574

$$\overline{Nu}_D = 1.13C_1 Re_{D,\max}^m Pr^{1/3} \tag{7.60}$$

$$\begin{bmatrix} N_L \geq 10 \\ 2000 \lesssim Re_{D,\max} \lesssim 40{,}000 \\ Pr \gtrsim 0.7 \end{bmatrix}$$

All properties appearing in the above equations are evaluated at the film temperature. If $N_L < 10$, a correction factor may be applied such that

$$\overline{Nu}_D\Big|_{(N_L<10)} = C_2\overline{Nu}_D\Big|_{(N_L\geq 10)} \tag{7.61}$$

where C_2 is given in Table 7.6.

The Reynolds number $Re_{D,\max}$ for the foregoing correlations is based on the *maximum fluid velocity* occurring within the tube bank. For the aligned arrangement, $V_{\max}$ occurs at the transverse plane A_1 of Figure 7.11*a*, and from the mass conservation requirement for an incompressible fluid

$$V_{\max} = \frac{S_T}{S_T - D}V \tag{7.62}$$

For the staggered configuration, the maximum velocity may occur at either the transverse plane A_1 or the diagonal plane A_2 of Figure 7.11*b*. It will occur at A_2 if the rows are spaced such that

$$2(S_D - D) < (S_T - D)$$

The factor of 2 results from the bifurcation experienced by the fluid moving from the A_1 to the A_2 planes. Hence $V_{\max}$ occurs at A_2 if

$$S_D = \left[S_L^2 + \left(\frac{S_T}{2}\right)^2\right]^{1/2} < \frac{S_T + D}{2}$$

in which case it is given by

$$V_{\max} = \frac{S_T}{2(S_D - D)}V \tag{7.63}$$

If $V_{\max}$ occurs at A_1 for the staggered configuration, it may again be computed from Equation 7.62.

TABLE 7.6 Correction factor C_2 of Equation 7.61 for $N_L < 10$ [20]

N_L	1	2	3	4	5	6	7	8	9
Aligned	0.64	0.80	0.87	0.90	0.92	0.94	0.96	0.98	0.99
Staggered	0.68	0.75	0.83	0.89	0.92	0.95	0.97	0.98	0.99

TABLE 7.7 Constants of Equation 7.64 for the tube bank in cross flow [15]

Configuration	$Re_{D,\max}$	C	m
Aligned	10–10^2	0.80	0.40
Staggered	10–10^2	0.90	0.40
Aligned	10^2–10^3	Approximate as a single (isolated) cylinder	
Staggered	10^2–10^3		
Aligned $(S_T/S_L > 0.7)^a$	10^3–2×10^5	0.27	0.63
Staggered $(S_T/S_L < 2)$	10^3–2×10^5	$0.35(S_T/S_L)^{1/5}$	0.60
Staggered $(S_T/S_L > 2)$	10^3–2×10^5	0.40	0.60
Aligned	2×10^5–2×10^6	0.021	0.84
Staggered	2×10^5–2×10^6	0.022	0.84

[a]For $S_T/S_L < 0.7$, heat transfer is inefficient and aligned tubes should not be used.

More recent results have been obtained and Zukauskas [15] has proposed a correlation of the form

$$\overline{Nu}_D = C\, Re_{D,\max}^m\, Pr^{0.36}\left(\frac{Pr}{Pr_s}\right)^{1/4} \tag{7.64}$$

$$\left[\begin{array}{l} N_L \geq 20 \\ 0.7 \lesssim Pr \lesssim 500 \\ 1000 \lesssim Re_{D,\max} \lesssim 2 \times 10^6 \end{array}\right]$$

where all properties except Pr_s are evaluated at the arithmetic mean of the fluid inlet and outlet temperatures and the constants C and m are listed in Table 7.7. The need to evaluate fluid properties at the arithmetic mean of the inlet ($T_i = T_\infty$) and outlet (T_o) temperatures is dictated by the fact that the fluid temperature will decrease or increase, respectively, due to heat transfer to or from the tubes. If the fluid temperature change, $|T_i - T_o|$, is large, significant error could result from evaluation of the properties at the inlet temperature. If $N_L < 20$, a correction factor may be applied such that

$$\overline{Nu}_D\big|_{(N_L<20)} = C_2\, \overline{Nu}_D\big|_{(N_L\geq 20)} \tag{7.65}$$

where C_2 is given in Table 7.8.

TABLE 7.8 Correction factor C_2 of Equation 7.65 for $N_L < 20$ ($Re_{D,\max} \gtrsim 10^3$) [15]

N_L	1	2	3	4	5	7	10	13	16
Aligned	0.70	0.80	0.86	0.90	0.92	0.95	0.97	0.98	0.99
Staggered	0.64	0.76	0.84	0.89	0.92	0.95	0.97	0.98	0.99

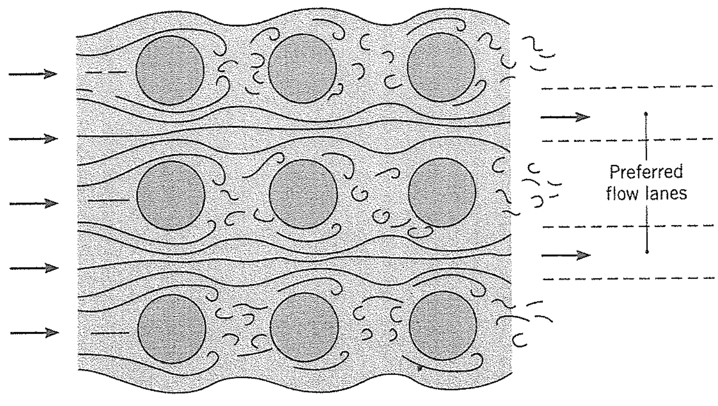

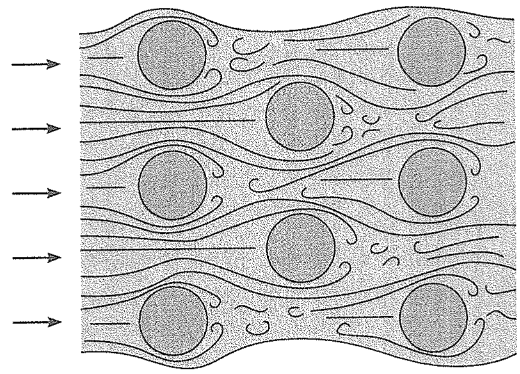

FIGURE 7.12 Flow conditions for (*a*) aligned and (*b*) staggered tubes.

Flow around tubes in the first row of a tube bank corresponds to that for a single (isolated) cylinder in cross flow. However, for subsequent rows, flow depends strongly on the tube bank arrangement (Figure 7.12). Aligned tubes beyond the first row are in the turbulent wakes of upstream tubes, and for moderate values of S_L convection coefficients associated with downstream rows are enhanced by turbulation of the flow. Typically, the convection coefficient of a row increases with increasing row number until approximately the fifth row, after which there is little change in the turbulence and hence in the convection coefficient. However, for small values of S_T/S_L, upstream rows, in effect, shield downstream rows from much of the flow, and heat transfer is adversely affected. That is, the preferred flow path is in lanes between the tubes and much of the tube surface is not exposed to the main flow. For this reason, operation of aligned tube banks with $S_T/S_L < 0.7$ (Table 7.7) is undesirable. For the staggered array, however, the path of the main flow is more tortuous and a greater portion of the surface area of downstream tubes remains in this path. In general, heat transfer enhancement is favored by the more tortuous flow of a staggered arrangement, particularly for small Reynolds number ($Re_D \lesssim 100$).

Since the fluid may experience a large change in temperature as it moves through the tube bank, the heat transfer rate could be significantly overpredicted by using $\Delta T = T_s - T_\infty$ as the temperature difference in Newton's law of cooling. As the fluid moves through the bank, its temperature approaches T_s and $|\Delta T|$ decreases. In Chapter 8 the appropriate form of ΔT is shown to be a *log-mean temperature difference*,

$$\Delta T_{\text{lm}} = \frac{(T_s - T_i) - (T_s - T_o)}{\ln\left(\dfrac{T_s - T_i}{T_s - T_o}\right)} \tag{7.66}$$

where T_i and T_o are temperatures of the fluid as it enters and leaves the bank, respectively. The outlet temperature, which is needed to determine ΔT_{lm}, may be estimated from

$$\frac{T_s - T_o}{T_s - T_i} = \exp\left(-\frac{\pi D N \bar{h}}{\rho V N_T S_T c_p}\right) \tag{7.67}$$

where N is the total number of tubes in the bank and N_T is the number of tubes in the transverse plane. Once ΔT_{lm} is known, the heat transfer rate per unit length of the tubes may be computed from

$$q' = N(\bar{h}\pi D \Delta T_{\text{lm}}) \tag{7.68}$$

The foregoing results may be used to determine mass transfer rates associated with evaporation or sublimation from the surfaces of a bank of cylinders in cross flow. Once again it is only necessary to replace $\overline{Nu}_D$ and Pr by $\overline{Sh}_D$ and Sc, respectively.

We close by recognizing that there is generally as much interest in the pressure drop associated with flow across a tube bank as in the overall heat transfer rate. The power required to move the fluid across the bank is often a major operating expense and is directly proportional to the pressure drop, which may be expressed as [15]

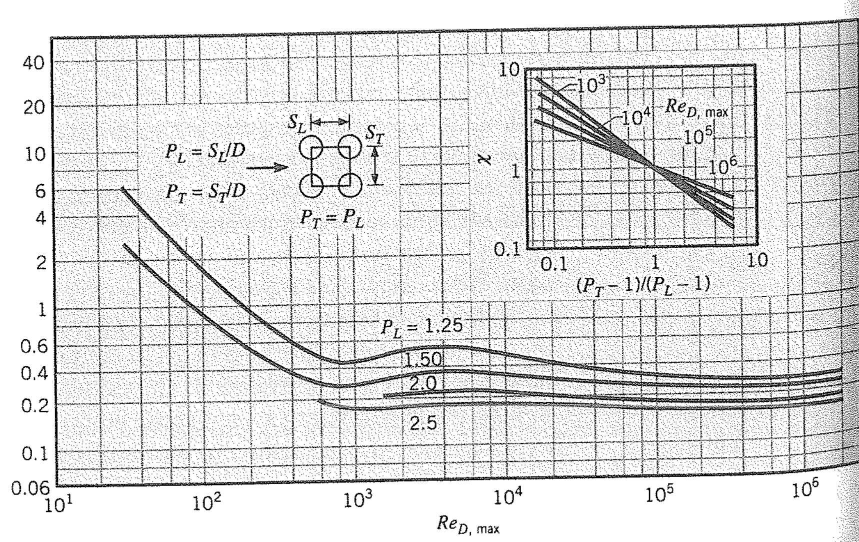

FIGURE 7.13 Friction factor f and correction factor χ for Equation 7.69. In-line tube bundle arrangement [15]. Used with permission.

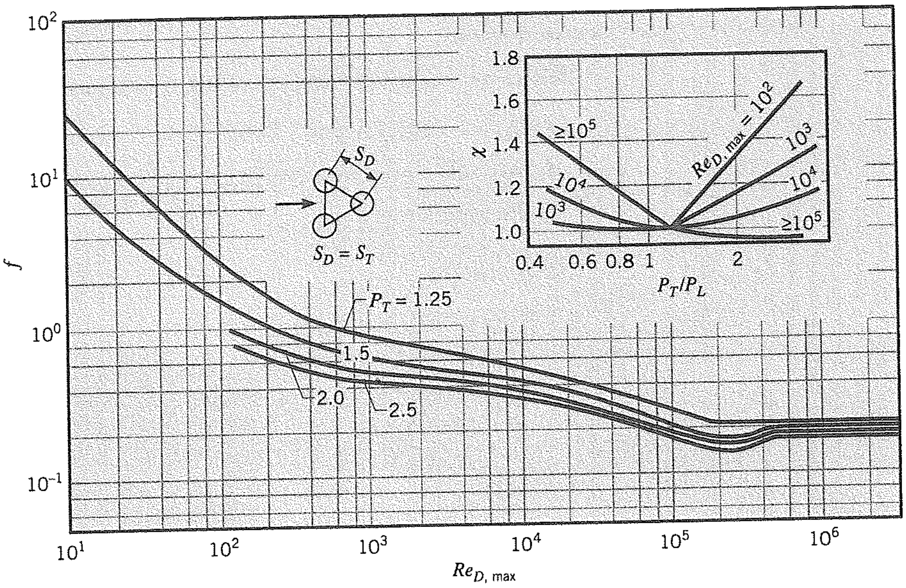

FIGURE 7.14 Friction factor f and correction factor χ for Equation 7.69. Staggered tube bundle arrangement [15]. Used with permission.

$$\Delta p = N_L \chi \left(\frac{\rho V_{max}^2}{2} \right) f \qquad (7.69)$$

The friction factor f and the correction factor χ are plotted in Figures 7.13 and 7.14. Figure 7.13 pertains to a square, in-line tube arrangement for which the dimensionless longitudinal and transverse pitches, $P_L \equiv S_L/D$ and $P_T \equiv S_T/D$, respectively, are equal. The correction factor χ, plotted in the inset, is used to apply the results to other in-line arrangements. Similarly, Figure 7.14 applies to a staggered arrangement of tubes in the form of an equilateral triangle ($S_T = S_D$), and the correction factor enables extension of the results to other staggered arrangements. Note that the Reynolds number appearing in Figures 7.13 and 7.14 is based on the maximum fluid velocity V_{max}.

EXAMPLE 7.7

Pressurized water is often available at elevated temperatures and may be used for space heating or industrial process applications. In such cases it is customary to use a tube bundle in which the water is passed through the tubes, while air is passed in cross flow over the tubes. Consider a staggered arrangement for which the tube outside diameter is 16.4 mm and the longitudinal and transverse pitches are $S_L = 34.3$ mm and $S_T = 31.3$ mm. There are seven rows of tubes in the airflow direction and eight tubes per row. Under typical operating conditions the cylinder surface temperature is at 70°C, while the air upstream temperature and velocity are 15°C and 6 m/s, respectively. Determine the air-side convection coefficient and the rate of heat transfer for the tube bundle. What is the air-side pressure drop?

Comments:

1. In using the energy balance of part 1 for the entire tube, properties (in this case, only c_p) are evaluated at $\overline{T}_m = (T_{m,0} + T_{m,L})/2$. However, in using the correlation for a local heat transfer coefficient, Equation 8.60, properties are evaluated at the local mean temperature, $T_{m,L} = 77°C$.
2. This problem is characterized neither by constant surface temperature nor by constant surface heat flux. It would therefore be erroneous to presume that the total heat loss from the tube is given by $q''_s(L)\pi DL = 717$ W. This result is substantially less than the actual heat loss of 1313 W because $q''_s(x)$ decreases with increasing x. This decrease in $q''_s(x)$ is due to reductions in both $h_x(x)$ and $[T_m(x) - T_\infty]$ with increasing x.

8.6 Convection Correlations: Noncircular Tubes and the Concentric Tube Annulus

Although we have thus far restricted our consideration to internal flows of circular cross section, many engineering applications involve convection transport in *noncircular tubes.* At least to a first approximation, however, many of the circular tube results may be applied by using *an effective diameter* as the characteristic length. It is termed the *hydraulic diameter* and is defined as

$$D_h \equiv \frac{4A_c}{P} \qquad (8.66)$$

where A_c and P are the *flow* cross-sectional area and the *wetted perimeter,* respectively. It is this diameter that should be used in calculating parameters such as Re_D and Nu_D.

For turbulent flow, which still occurs if $Re_D \gtrsim 2300$, it is reasonable to use the correlations of Section 8.5 for $Pr \gtrsim 0.7$. However, in a noncircular tube the convection coefficients vary around the periphery, approaching zero in the corners. Hence in using a circular tube correlation, the coefficient is presumed to be an average over the perimeter.

For laminar flow, the use of circular tube correlations is less accurate, particularly with cross sections characterized by sharp corners. For such cases the Nusselt number corresponding to fully developed conditions may be obtained from Table 8.1, which is based on solutions of the differential momentum and energy equations for flow through the different duct cross sections. As for the circular tube, results differ according to the surface thermal condition. Nusselt numbers tabulated for a uniform surface heat flux presume a constant flux in the axial (flow) direction, but a constant temperature around the perimeter at any cross section. This condition is typical of highly conductive tube wall materials. Results tabulated for a uniform surface temperature apply when the temperature is constant in both the axial and peripheral directions.

Although the foregoing procedures are generally satisfactory, exceptions do exist. Detailed discussions of heat transfer in noncircular tubes are provided in several sources [11, 12, 24].

TABLE 8.1 Nusselt numbers and friction factors for fully developed laminar flow in tubes of differing cross section

		$Nu_D \equiv \frac{hD_h}{k}$		
Cross Section	$\frac{b}{a}$	(Uniform q_s'')	(Uniform T_s)	$f\,Re_{D_h}$
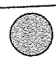	—	4.36	3.66	64
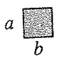	1.0	3.61	2.98	57
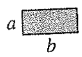	1.43	3.73	3.08	59
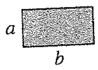	2.0	4.12	3.39	62
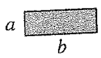	3.0	4.79	3.96	69
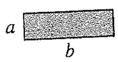	4.0	5.33	4.44	73
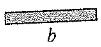	8.0	6.49	5.60	82
	∞	8.23	7.54	96
Heated 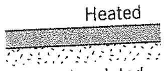 Insulated	∞	5.39	4.86	96
	—	3.11	2.49	53

Used with permission from W. M. Kays and M. E. Crawford, *Convection Heat and Mass Transfer*, 3rd ed. McGraw-Hill, New York, 1993.

Many internal flow problems involve heat transfer in a *concentric tube annulus* (Figure 8.11). Fluid passes through the space (annulus) formed by the concentric tubes, and convection heat transfer may occur to or from both the inner and outer tube surfaces. It is possible to independently specify the heat flux or temperature,

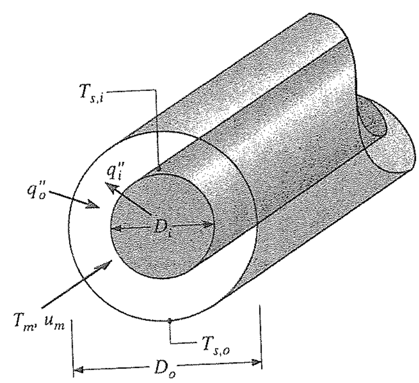

FIGURE 8.11
The concentric tube annulus.

that is, the thermal condition, at each of these surfaces. In any case the heat flux from each surface may be computed with expressions of the form

$$q_i'' = h_i(T_{s,i} - T_m) \tag{8.67}$$

$$q_o'' = h_o(T_{s,o} - T_m) \tag{8.68}$$

Note that separate convection coefficients are associated with the inner and outer surfaces. The corresponding Nusselt numbers are of the form

$$Nu_i \equiv \frac{h_i D_h}{k} \tag{8.69}$$

$$Nu_o \equiv \frac{h_o D_h}{k} \tag{8.70}$$

where, from Equation 8.66, the hydraulic diameter D_h is

$$D_h = \frac{4(\pi/4)(D_o^2 - D_i^2)}{\pi D_o + \pi D_i} = D_o - D_i \tag{8.71}$$

For the case of fully developed laminar flow with one surface insulated and the other surface at a constant temperature, Nu_i or Nu_o may be obtained from Table 8.2. Note that in such cases we would be interested only in the convection coefficient associated with the isothermal (nonadiabatic) surface.

If uniform heat flux conditions exist at both surfaces, the Nusselt numbers may be computed from expressions of the form

$$Nu_i = \frac{Nu_{ii}}{1 - (q_o''/q_i'')\theta_i^*} \tag{8.72}$$

$$Nu_o = \frac{Nu_{oo}}{1 - (q_i''/q_o'')\theta_o^*} \tag{8.73}$$

The influence coefficients (Nu_{ii}, Nu_{oo}, θ_i^*, and θ_o^*) appearing in these equations may be obtained from Table 8.3. Note that q_i'' and q_o'' may be positive or negative, depending on whether heat transfer is to or from the fluid, respectively. Moreover, situations may arise for which the values of h_i and h_o are negative. Such results,

TABLE 8.2 Nussult number for fully developed laminar flow in a circular tube annulus with one surface insulated and the other at constant temperature

D_i/D_o	Nu_i	Nu_o	*Comments*
0	—	3.66	See Equation 8.55
0.05	17.46	4.06	
0.10	11.56	4.11	
0.25	7.37	4.23	
0.50	5.74	4.43	
≈1.00	4.86	4.86	See Table 8.1, $b/a \rightarrow \infty$

Used with permission from W. M. Kays and H. C. Perkins, in W. M. Rohsenow and J. P. Hartnett, Eds., *Handbook of Heat Transfer,* Chap. 7, McGraw-Hill, New York, 1972.

TABLE 8.3 Influence coefficients for fully developed laminar flow in a circular tube annulus with uniform heat flux maintained at both surfaces

D_i/D_o	Nu_{ii}	Nu_{oo}	θ_i^*	θ_o^*
0	—	4.364	∞	0
0.05	17.81	4.792	2.18	0.0294
0.10	11.91	4.834	1.383	0.0562
0.20	8.499	4.833	0.905	0.1041
0.40	6.583	4.979	0.603	0.1823
0.60	5.912	5.099	0.473	0.2455
0.80	5.58	5.24	0.401	0.299
1.00	5.385	5.385	0.346	0.346

Used with permission from W. M. Kays and H. C. Perkins, in W. M. Rohsenow and J. P. Hartnett, Eds., *Handbook of Heat Transfer,* Chap. 7, McGraw-Hill, New York, 1972.

when used with the sign convention implicit in Equations 8.67 and 8.68, reveal the relative magnitudes of T_s and T_m.

For fully developed turbulent flow, the influence coefficients are a function of the Reynolds and Prandtl numbers [24]. However, to a first approximation the inner and outer convection coefficients may be assumed to be equal, and they may be evaluated by using the hydraulic diameter, Equation 8.71, with the Dittus–Boelter equation, Equation 8.60.

8.7 *Heat Transfer Enhancement*

Several options are available for enhancing heat transfer associated with internal flows. Enhancement may be achieved by increasing the convection coefficient and/or by increasing the convection surface area. For example, h may be increased by introducing surface roughness to enhance turbulence, as, for example, through machining or insertion of a coil-spring wire. The wire insert (Figure 8.12*a*) provides a helical roughness element in contact with the tube inner surface. Alternatively, the convection coefficient may be increased by inducing swirl through insertion of a twisted tape (Figure 8.12*b*). The insert consists of a thin strip that is periodically twisted through 360°. Introduction of a tangential velocity component increases the speed of the flow, particularly near the tube wall. The heat transfer area may be increased by manufacturing a tube with a grooved inner surface (Figure 8.12*c*), while both the convection coefficient and area may be increased by using spiral fins or ribs (Figure 8.12*d*). In evaluating any heat transfer enhancement scheme, attention must also be given to the attendant increase in pressure drop and hence fan or pump power requirements. Comprehensive assessments of enhancement options have been published [25–28], and the *Journal of Enhanced Heat Transfer* provides access to recent developments in the field.

By coiling a tube (Figure 8.13), heat transfer may be enhanced without turbulence or additional heat transfer surface area. In this case, centrifugal forces within